Optimization of Virus Yield as a Strategy to Increase the Efficiency of Rabies Vaccine by BHK-21 Cells in a Bioreactor

Seyed Dawood Mousavi-Nasab [1], Alireza Gholami [2], Nayeb Ali Ahmadi [3, 4], Rajab Mardani [5], Delaram Doroud [2], Nima Naseri [6], Fatemeh Zali [7], Golshid Javdani [2, *] and Maryam Shahali [5, **]

[1]National Reference Laboratory, Department of Arboviruses and Viral Hemorrhagic Fevers, Pasteur Institute of Iran, Tehran, Iran
[2]Department of Research and Production Complex, Pasteur Institute of Iran, Tehran, Iran
[3]Proteomics Research Center, Faculty of Paramedical Sciences, Shahid Beheshti University of Medical Sciences, Tehran, Iran
[4]Department of Medical Lab Technology, Proteomics Research Center, Faculty of Paramedical Sciences, Shahid Beheshti University of Medical Sciences, Tehran, Iran
[5]Department of Viral Vaccines, Research and Production Complex, Pasteur Institute of Iran, Tehran, Iran
[6]Department of Clinical Biochemistry, Hamadan University of Medical Sciences, Hamadan, Iran
[7]Department of Clinical Biochemistry, Faculty of Medicine, Tehran University of Medical Sciences, Tehran, Iran

[*]*Corresponding author*: Department of Research and Production Complex, Pasteur Institute of Iran, Tehran, Iran. Email: golshidjavdani@gmail.com
[**]*Corresponding author*: Department of Viral Vaccines, Research and Production Complex, Pasteur Institute of Iran, Tehran, Iran. Email: maryam.shahali@gmail.com

Abstract

Background: Rabies is a usually fatal viral zoonotic and preventable disease. The efficacy and safety of animal rabies vaccination made in permanent BHK-21 cell culture have been proven over a long period of use. By increasing the yield of cells and viruses, the efficacy of the vaccine can be increased.

Objectives: The objective of this study was to optimize and maximize the output of a rabies vaccine made on BHK cells in a bioreactor.

Methods: This study examined the impacts of independent parameters, such as pH, temperature, cell density, and dissolved oxygen (DO), on rabies virus strain PV-PARIS yield for a central composite design. To achieve high viral production, this study used the central composite approach to optimize cell development.

Results: The findings showed that BHK-21 cells were grown under the ideal conditions of pH 7.21, temperature 35.05°C, 68.75% for DO, and 2.30×10^6 cell/mL of cell density to produce high titers of rabies virus (4.7×10^7 plaque-forming unit [PFU]/mL). High correlation coefficients (0.927) validated that the predicted model was well-fitted with the data, and the statistical analysis of the collected data indicated that the experimental data and predicted model were well-matched. The accuracy of this model's predictions was correlated with values of adjusted R-squared (R^2_{Adj}) and predicted R-squared (R^2_{Pred}).

Conclusions: These upgrades lead to a more reliable and economical procedure that makes industrialization and commercialization easier.

Keywords: Rabies Vaccine, Bioreactor, Cell Counts, Optimization

1. Background

The Lyssavirus genus and Rhabdoviridae family of viruses, which includes the rabies virus, are responsible for the zoonotic disease known as rabies (1). Taxonomically, lyssaviruses are categorized according to changes in nucleoprotein antigens. The first of the six genotypes is represented by the rabies virus. In more than 150 nations, rabies is expected to claim the lives of 59,000 individuals annually, with 95% of cases happening in Africa and Asia (2). Due to extensive underreporting and hazy estimations, this number probably underestimates the true burden of

the disease (3).

Ninety-nine percent of human cases of rabies are brought on by dog bites, which are the disease's most prevalent reservoir and vector. The most cost-effective method of preventing rabies in humans is by immunizing dogs (4). Iran has a vaccination program that is the first choice for containing and eradicating the rabies virus. The program is supported by other initiatives to ascertain whether it is effective, such as surveys following vaccination, bite reporting, and cold chain management, in addition to a targeted elimination program that

considers animal welfare, proper veterinary medication handling, and a coordination system (5).

In affluent nations, rabies vaccinations based on MRC-5 cells, a human fibroblast cell line, Vero cells, a continuous vervet monkey kidney cell line, and baby hamster kidney fibroblasts (BHK cells), heteroploid cells, are already accessible (4). Due to their productivity for rabies virus growth and their capacity to grow in suspension in large-scale bioreactors, a number of cell lines, including the permanent BHK-21 cell line, have been regarded as promising candidates for producing efficient cell-based rabies vaccines at a reasonable cost (5, 6). Optimizing viral productivity is a different method for creating a low-cost rabies cell-culture vaccine (7). By enhancing the upstream process' productivity, this technique increases the number of vaccine doses produced per run (8).

There are various methods that can be applied to optimize a process. The traditional optimization strategy entails individually testing each process variable (9). This necessitates the execution of numerous expensive and time-consuming experiments. One of the most important considerations in the design of experiment technique is choosing an appropriate experimental design. Numerous studies in the literature discuss the traits of the most popular experimental designs. The most popular choice for a response surface planned experiment is a central composite design (CCD).

By adding center and axial points to an existing factorial design, we can effectively estimate first- and second-order terms and model a response variable with curvature using a CCD. A central composite method, however, employs numerous progressive tests to analyze numerous elements concurrently and swiftly pinpoint the crucial ones. As an illustration, a CCD in 2016 optimized the growth and biomass production of Haemophilus influenza type B (8). The optimal combination that will result in the best performance is then predicted using these control factors. One of the advantages of cell culture-based rabies vaccines is their safety.

2. Objectives

The objective of this study was to maximize the output of an animal rabies vaccine made on BHK cells. To achieve high viral production, this study used the central composite approach to optimize cell development.

3. Methods

3.1. Cell Line and Culture Media

The BHK-21 cell line (baby hamster kidney) and 5% fetal bovine serum (FBS) (Life Technologies, USA) with Dulbecco's Modified Eagle's Medium (DMEM) (Life Technologies, USA) with 2.5 g/L bicarbonate were used for cell culture, which was obtained from the Cell Bank Department of Pasteur Institute of Iran. It was previously tested for the absence of mycoplasma. The inoculated cells were incubated at 37°C with 5% CO_2.

3.2. Growth Assay

In this study, 250 mL spinner flasks with 200 mL of cultured cells and an initial concentration of 3×10^7 cells per mL were used for the cultures, which were carried out at 37°C in an incubator with 5% CO_2 and 37°C. The cells were grown in DMEM supplemented with 0.2 mM for each of serine and methionine and 10% FBS. Samples were taken daily to measure cell concentration. The stirring speed was maintained at 30 rpm.

3.3. Cell Counting

The BHK-21 cells grown in clumps were trypsinized and counted in the presence of 0.2% trypan blue. The exponential growth function was used to calculate the specific growth rate as follows:

$$\mu = (lnX_2 - lnX_1) / (t_1 - t_2) \tag{1}$$

Where X denotes the viable cell density per mL (sampling is taken every 1 hour), and t is the time points expressed in hours.

3.4. Virus Strain and Cell Infection

The PV-PARIS/BHK strain is used to create veterinary vaccines. It was developed from the PV-CEPANZO strain of stable rabies, which was first serially transmitted through young rabbits (PV-PARIS). The PV-PARIS fixed rabies virus 93127 FRA was obtained for this purpose from the Institut Pasteur in Paris, France, and used to infect BHK-21 C-13 cells. The PV-PARIS rabies virus strain was introduced into BHK-21 cells with a cell density of 1×10^6 cells/mL and an infection multiplicity of 0.1 cells, and they passed the initial infection stage for 2 hours in a shaker incubator.

3.5. Bioreactor Cultures

For this purpose, a 10-liter bioreactor (Inceltech, Toulouse, France) was used, in which Spanner flask cells that have passed the initial stage of infection are injected into the bioreactor. The infection proliferation stage was carried out under the following conditions:

Temperature 37°C, pH 7.1, air saturation at 70%, and stirring conditions at 40 rpm

In this case, daily samples were collected to measure cell count and cell viability, virus titer, and infection.

3.6. Bioprocess Optimization Using Design-of-Experiments Methodology

The statistical design of the experiments was used to optimize operational parameters of viral yield for BHK cells producing rabies vaccine in a bioreactor where the parameters dissolved oxygen (DO), cell density, temperature, and pH are measured.

3.7. Rabies Virus Titration

In order to compare the production quantity of the modified virus, its titer is evaluated in comparison to the titer of the original virus. In this method, rabies virus suspension in cell culture can be measured by the focus forming assay. Therefore, in this method, the antibody attached to the fluorescent material is attached to each virus particle and can be detected within 24 hours, and the virus titer is expressed as Fluorescent Focus Units (FFU/mL). Briefly, several serial dilutions of the virus are inoculated into the cell culture in duplicate, and the number of FFU of each dilution is counted after 24 hours. In this method, first, in a cell culture flask, BSR cells are cultured, and the cell suspension is prepared with the accumulation of 1 million cells per milliliter. Additionally, successive one-tenth dilutions are prepared from the viral solution in test tubes. In an eight-well Lab-Tek slide, 200 microliters of cell suspension, equivalent to 200,000 cells, are added to each well, and then 100 microliters of each virus dilution are added to each well. The resulting slide is placed at 37 degrees for 24 hours. Then, the liquid on top of the cells is removed and poured into a waste container containing disinfectants. In the next step, Lab-Tek lamella is washed with phosphate-buffered saline (PBS). The slide is placed in a container containing cold pure acetone for 30 minutes. The amount of 25 microliters of rabies virus anti-nucleocapsid antibody conjugated with fluorescein isothiocyanate (FITC) is poured on all areas with cells and placed at 37 degrees for one hour. Finally, the slides are studied using an ultraviolet (UV) microscope. The calculation of initial virus concentration is done using the following formula:

The number of cells containing viral particles in the well × the dilution factor × 10 = The number of viruses (per milliliter of the initial solution)

3.8. Plaque Assay for Infectivity

To determine the number of plaque-forming units (PFUs), serially diluted in vitro reaction mixtures were used by standard methods (Rueckert and Pallansch, 1981). Briefly, first, BHK-21 cells are grown to confluency on 60-mm Petri dishes and, therefore, exposed to the serial dilutions of the virus that are made up of DMEM containing 2% FBS (0.25 mL) for 30 minutes at room temperature. Finally, the cells are covered with 2.5 mL of medium containing 0.6% Noble agar (prepared in a 44°C water bath), and plaques are allowed to grow at 37°C and 5% CO_2 for 26 hours. The cell monolayers are stained with 0.1% crystal violet in 20% ethanol, and after washing the dishes with water, the plaques appear as transparent spots (typically 1 to 2 mm in diameter) on a blue background of cells.

3.9. Virus Harvest Inactivation

After 72 hours, the bioreactor's supernatant containing the grown virus was collected and cleared by low-speed centrifugation for 15 minutes at 3000 g, removing cell debris. This was subsequently deactivated by beta-propiolactone (BPL) (HiMedia, India). Because the complete inactivation of the rabies virus can be achieved at this dilution without lowering the antigenicity properties of the rabies vaccine, the final concentration of the BPL used was 1/3000. Additionally, the deoxyribonucleic acid (DNA) of the remaining cell is sufficiently broken and inactivated at this dilution (Laboratory techniques in rabies).

3.10. Statistical Analysis and Model Validation

The CCD experiment generated all of the data, which were then submitted to multiple regression analysis using least squares to create the regression models. To fit the data, a second-order (quadratic) function was applied. Utilizing Design Expert 13 statistical software, several tasks, including experimental design, data analysis, interaction plotting, and factor condition optimization, were completed. Predicted responses were plotted against experimentally derived data in Excel 2019 to confirm model fits. A P-value less than 0.05 was considered significant.

4. Results

4.1. Central Composite Analysis

Several experiments were carried out using the CCD technique to examine the impact of process variables (i.e., pH, cell density, DO, and temperature) on virus yield optimization (Tables 1 and 2). According to the data in Tables 1 and 2, the amount of response PFU was also calculated, as shown in Table 3. A second-order polynomial equation of coded units was expressed based on the CCD and input variables to show relationships between the responses and independent parameters.

4.2. Cell Infection

To check cell infection, the immunofluorescence method was used, and by using rabies nucleocapsid, the ratio of infected to uninfected cells was observed and reported as a percentage (Figure 1).

Table 1. Experimental Parameters and Their Levels in a Central Composite Design

Symbol	Factors	Range
X_1	pH	7.17 - 7.31
X_2	Temperature (°C)	34.70 - 36.10
X_3	Dissolved oxygen (DO) (%)	67.80 - 71.50
X_4	Cell density (cell/mL)	1.7×10^6 - 2.50×10^6

Table 2. Central Composite Design Matrix

No	Factors			
	pH	Temperature (°C)	DO (%)	Cell Density (Cell/mL)
1	7.21	35.75	70.58	1.90×10^6
2	7.21	35.05	70.58	1.90×10^6
3	7.24	35.40	69.65	2.10×10^6
4	7.28	35.75	70.58	1.90×10^6
5	7.28	35.75	70.58	2.30×10^6
6	7.24	35.40	67.80	2.10×10^6
7	7.21	35.05	68.72	2.30×10^6
8	7.28	35.05	68.72	2.30×10^6
9	7.24	35.40	69.65	2.10×10^6
10	7.24	35.40	69.65	2.10×10^6
11	7.28	35.75	68.72	1.90×10^6
12	7.24	35.40	69.65	1.70×10^6
13	7.21	35.05	70.58	2.30×10^6
14	7.21	35.05	68.72	1.90×10^6
15	7.21	35.75	68.72	1.90×10^6
16	7.28	35.75	68.72	2.30×10^6
17	7.21	35.75	70.58	2.30×10^6
18	7.24	36.10	69.65	2.10×10^6
19	7.24	35.40	69.65	2.10×10^6
20	7.28	35.05	70.58	1.90×10^6
21	7.24	34.70	69.65	2.10×10^6
22	7.24	35.40	69.65	2.10×10^6
23	7.21	35.75	68.72	2.30×10^6
24	7.28	35.05	70.58	2.30×10^6
25	7.24	35.40	69.65	2.50×10^6
26	7.31	35.40	69.65	2.10×10^6
27	7.24	35.40	69.65	2.10×10^6
28	7.17	35.40	69.65	2.10×10^6
29	7.28	35.05	68.72	1.90×10^6
30	7.24	35.40	71.50	2.10×10^6

Abbreviations: No, number of experiments; DO, dissolved oxygen.

Table 3. Central Composite Design Matrix with Response [a]

No	Factors				Response (PFU/mL)
	X_1	X_2	X_3	X_4 (Cell/mL)	
1	7.21	35.75	70.58	1.90×10^6	4.1×10^7
2	7.21	35.05	70.58	1.90×10^6	3.8×10^7
3	7.24	35.40	69.65	2.10×10^6	4.1×10^7
4	7.28	35.75	70.58	1.90×10^6	4.0×10^7
5	7.28	35.75	70.58	2.30×10^6	3.8×10^7
6	7.24	35.40	67.80	2.10×10^6	4.0×10^7
7	7.21	35.05	68.72	2.30×10^6	4.7×10^7
8	7.28	35.05	68.72	2.30×10^6	4.4×10^7
9	7.24	35.40	69.65	2.10×10^6	4.1×10^7
10	7.24	35.40	69.65	2.10×10^6	4.2×10^7
11	7.28	35.75	68.72	1.90×10^6	3.7×10^7
12	7.24	35.40	69.65	1.70×10^6	3.6×10^7
13	7.21	35.05	70.58	2.30×10^6	4.2×10^7
14	7.21	35.05	68.72	1.90×10^6	4.2×10^7
15	7.21	35.75	68.72	1.90×10^6	3.6×10^7
16	7.28	35.75	68.72	2.30×10^6	4.1×10^7
17	7.21	35.75	70.58	2.30×10^6	4.5×10^7
18	7.24	36.10	69.65	2.10×10^6	4.3×10^7
19	7.24	35.40	69.65	2.10×10^6	4.4×10^7
20	7.28	35.05	70.58	1.90×10^6	4.0×10^7
21	7.24	34.70	69.65	2.10×10^6	4.5×10^7
22	7.24	35.40	69.65	2.10×10^6	4.3×10^7
23	7.21	35.75	68.72	2.30×10^6	4.3×10^7
24	7.28	35.05	70.58	2.30×10^6	3.7×10^7
25	7.24	35.40	69.65	2.50×10^6	4.1×10^7
26	7.31	35.40	69.65	2.10×10^6	4.1×10^7
27	7.24	35.40	69.65	2.10×10^6	4.3×10^7
28	7.17	35.40	69.65	2.10×10^6	4.5×10^7
29	7.28	35.05	68.72	1.90×10^6	4.2×10^7
30	7.24	35.40	71.50	2.10×10^6	3.9×10^7

Abbreviation: PFU, Plaque-forming unit.

[a] Cell density (X4), dissolved oxygen (DO) (X3), pH (X1), and temperature (X2) were among these variables. Design Expert 13 software was used to implement the central composite design with response surface methodology (RSM) with four factorial points and four independent variables in order to statistically improve the virus yield process.

4.3. Analysis of Variance Parameters: Cell Density, Dissolved Oxygen, pH, and Temperature

The results of the analysis of variance for the model are shown in Table 4. The importance of each parameter is determined by the F-value and P-value. In this model, all the parameters except X_1X_2, X_1X_3, X_2X_4, X_1^2, and X_2^2 have values less than 0.05 and are significant.

Lack of Fit is the other important parameter that expresses the fraction of the sum of squares remaining, which occurs due to the inefficiency of the model. A good non-fit model should have a low value. The difference with the response's P-value of 0.7575 shows that the second-order equation suggested for this project is valid.
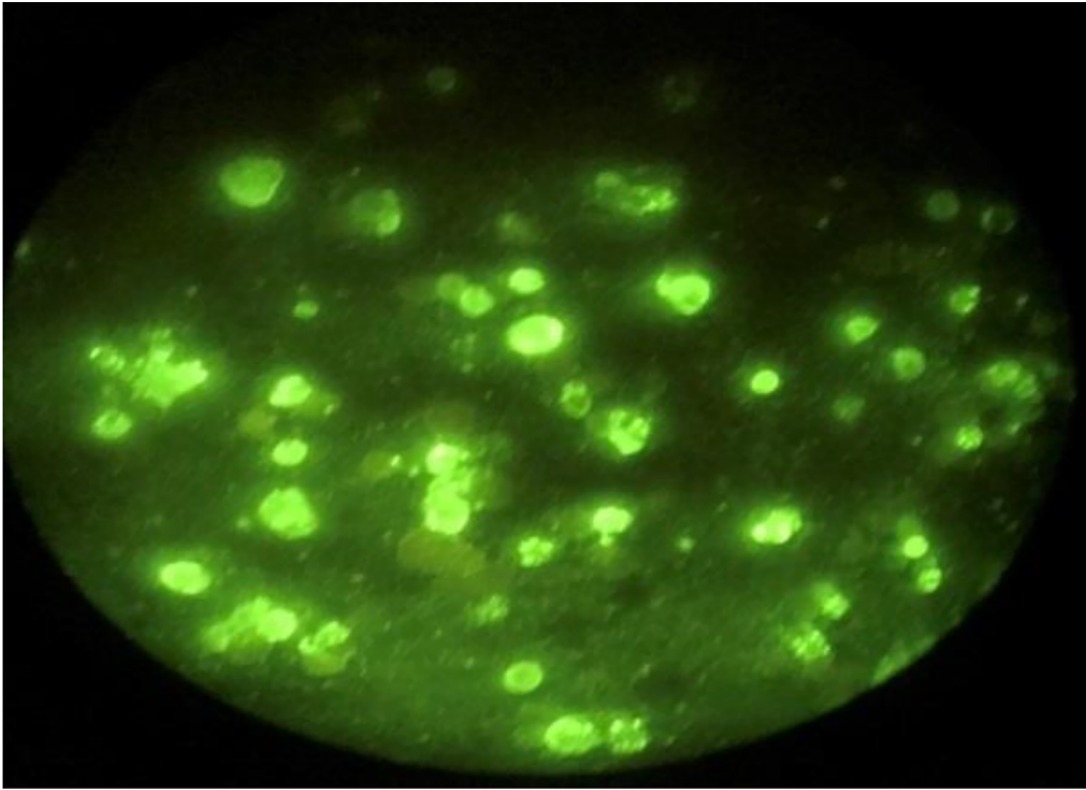
Figure 1. Infected cells observed in green color by immunofluorescence method.

4.4. Regression Analysis

It is necessary to investigate some statistical parameters before introducing the fitting model. The correlation coefficient (R-squared [R^2]) is a measure of the fitting of the predicted model with the data resulting from the experiments. The adjusted R-squared (R^2_{Adj}) or the corrected correlation coefficient, such as R^2, is an indicator for showing the model's usefulness; however, more precisely, it considers degrees of freedom. The strength of the model is predicted to be examined using the predicted residual error sum of squares (PRESS), where the lower the parameter, the more sensitive the model is to its positive data. The predicted R-squared (R^2_{Pred}), or the predicted correlation coefficient, is a combination of the PRESS and R^2, and the higher the value is, the more powerful the model will be. The signal-to-noise ratio of the model, which should be greater than 4 for the model under consideration, indicates that the model is accurate enough (10).

A quadratic model has been selected to predict the response, as shown in Table 5. The high correlation coefficient (0.9278) in this model confirms that the predicted model closely matches the data.

The values of R2Adj and R2Pred were accurately obtained in this model, and their closeness to 1 indicates a good relationship between the experimental results and the expected results. The anticipated model has a low PRESS value (0.63), which represents the sensitivity and power of the model. In addition, the model's adequate precision is 15.546 > 4, which denotes a favorable signal-to-noise ratio. On the other hand, the high accuracy of the expressed model is expressed by the low value for the model's standard deviation (0.61).

4.5. Diagnostic Tools

In addition to statistical parameters, there are several diagnostic instruments to demonstrate the suitability of the anticipated model as follows:

(1) Typical layout: The assumption that the error follows a standard button is a fundamental one in statistics. In order to verify this presumption, the test data are fitted with the normal probability curve. The error follows the normal distribution if the distribution is far from the S-shaped distribution. A normal probability curve is depicted in Figure 2A, in which the distribution of the residuals has a normal distribution and is relatively close to the reference line.

Table 4. Analysis of Variance of Quadratic Response Level

Source	Sum of Squares	DF	Mean of Squares	F-Value	P-Value
Model	2.11	14	0.15	13.77	< 0.0001
x_1	0.22	1	0.22	20.14	0.0004
x_2	0.094	1	0.094	8.57	0.0104
x_3	0.070	1	0.070	6.43	0.0228
x_4	0.40	1	0.40	36.59	< 0.0001
x_1x_2	0.0056	1	0.0056	0.51	0.4844
x_1x_3	0.031	1	0.031	2.80	0.1151
x_1x_4	0.23	1	0.23	20.62	0.0004
x_2x_3	0.39	1	0.39	35.69	< 0.0001
x_2x_4	0.016	1	0.016	1.43	0.2507
x_3x_4	0.14	1	0.14	12.85	0.0027
X_1^2	0.0024	1	0.0024	0.22	0.4456
X_2^2	0.032	1	0.032	2.96	0.1058
X_3^2	0.17	1	0.17	15.30	0.0014
X_4^2	0.29	1	0.29	26.65	0.0001
Residual	0.16	15	0.011		
Lack of fit	0.091	10	9.083E - 003	0.62	0.7575
Pure error	0.073	5	0.015		
Cor total	2.27	29			

Table 5. Statistical Parameters Considered to Prove the Adequacy of the Quadratic Model

Model	R^2	R^2_{Adj}	R^2_{Pred}	PRESS	SD
Quadratic	0.9278	0.8604	0.7234	0.63	0.610

Abbreviations: R^2, R-squared; R^2_{Adj}, adjusted R-squared; R^2_{Pred}, predicted R-squared; PRESS, predicted residual error sum of squares; SD, standard deviation.

(2) The residuals versus expected plot aims to investigate the systematic nature or prevalence of errors. If the residuals are systematic, it is a warning to re-examine the trial and possibly repeat it. If the residuals are random, it indicates that the tests were correct. The presence of the remaining on both the positive and negative sides indicates that the experiment did not contain any systematic errors.

(3) If residuals versus run plot exhibits a specific trend (uptrend or downtrend), it is indicative of a mistake. As can be seen in Figure 1C, this plot lacks a clear pattern for the expected model.

(4) The predicted versus actual plot shows how experimental results and predicted model outcomes relate to one another; the closer the data are to the bisector model, the more significant the model's influence is. This plot also adheres to the normal distribution, as seen in Figure 2D.

4.6. Interaction Between Parameters

The relationships between the factors are depicted via three-dimensional (3D) and contour charts. The relationship between temperature and pH parameters has an impact on the reaction (Figure 3).

When pH and DO are held constant at their midpoints, the effect of DO (%) and cell density (cell/mL) parameters on the response is shown in Figure 4. The parameters' contour plot shows that the highest response occurs at a cell density of 2.30×10^6 cells per milliliter.

4.7. Optimization of Independent Variables and Validation Experiment

In Table 6, the ideal circumstances for a full response are listed. As can be seen, at pH 7.21, temperature 35.05°C, DO 68.75%, and cell density 2.30×10^6 cell/mL with desirability of 1, the maximum response of 4.7×10^7 PFU/mL occurs (Table 6).
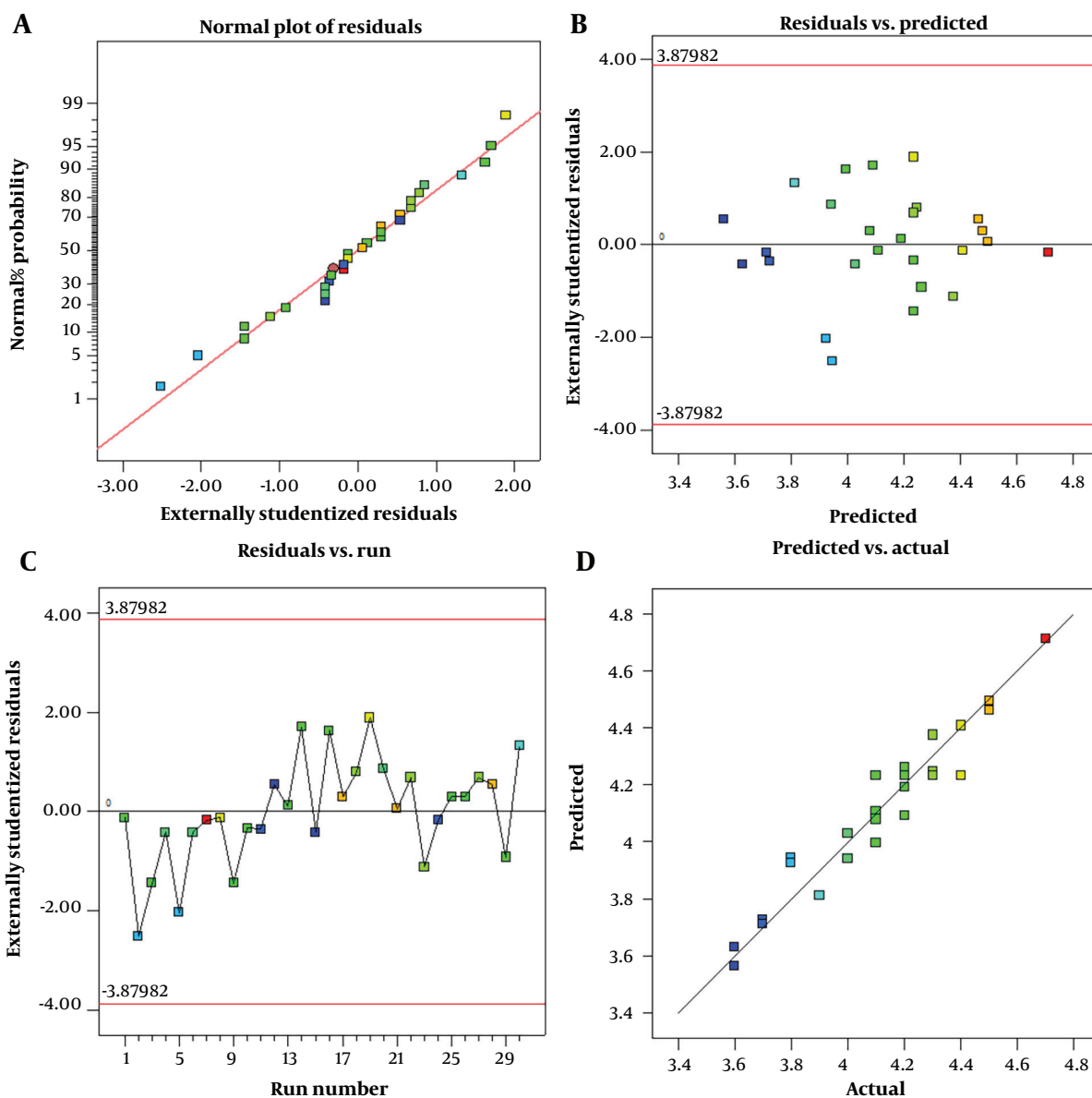
Figure 2. Checking statistical parameters: (A) Normal probability plot, (B) residuals versus prediction plot, (C) residuals versus run plot, and (D) predicted versus actual plot.

The response was carried out four times experimentally under these conditions to determine the model's accuracy in predicting the ideal conditions, and a value of 4.7×10^7 PFU/mL was obtained. It stands for this model's strong capacity for estimation and prediction.

5. Discussion

As previously stated, the huge public health problem posed by rabies caused by wild animals can only

be resolved by educating a willing community and encouraging them to internalize and use preventative measures. The production of an effective vaccine is a key idea [11]. Currently, homogenous systems, such as bioreactors, or heterogeneous systems, such as roller flasks and roller bottles, are used to produce products made from cell cultures, such as therapeutic proteins, viral vaccines, and monoclonal antibodies. The majority of the procedures are completed in batch culture mode and multiple flasks [12].
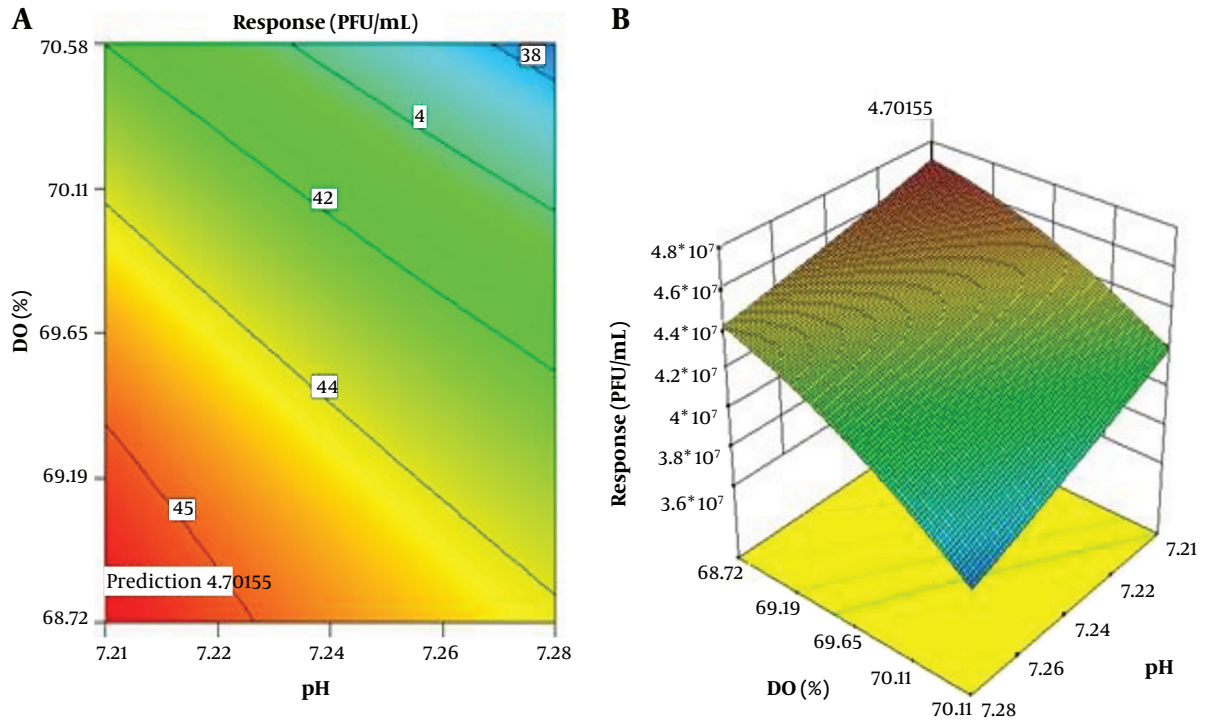
Figure 3. (A) Contour and (B) three-dimensional (3D) plot for the effects of pH and dissolved oxygen (DO) (%) parameters on the response.
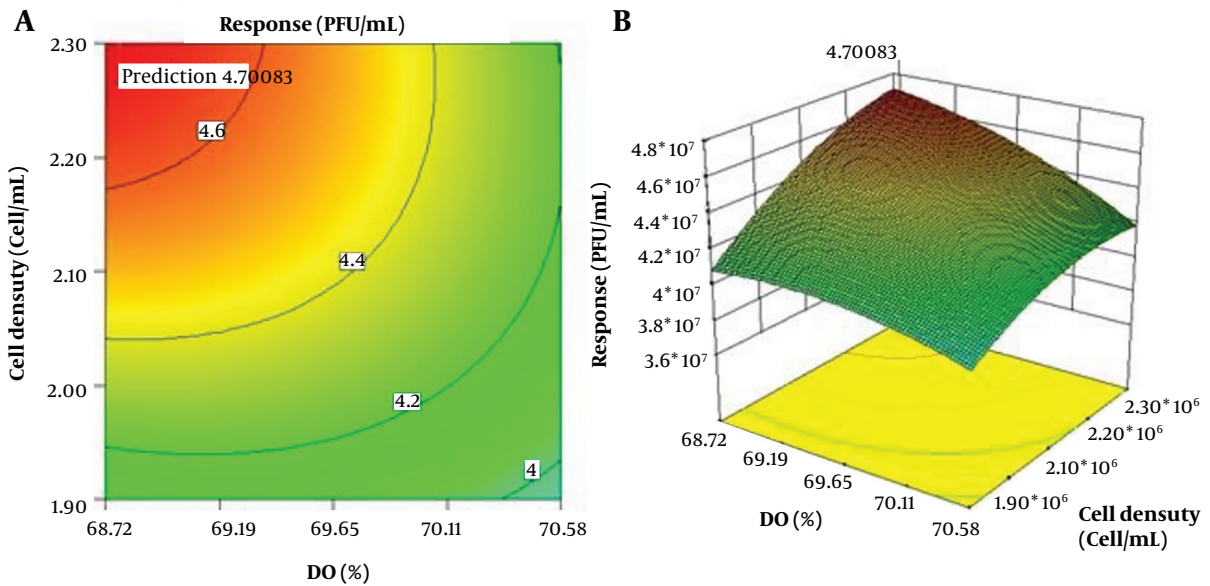
Figure 4. (A) Contour and (B) three-dimensional (3D) plot for the effect of dissolved oxygen (DO) (%) and cell density (cell/mL) on the response.

Table 6. Results for Optimization of Independent Variables and Validation of Experiments

Variables	Values
Optimum factor	
pH	7.21
Temperature (°C)	35.05
DO (%)	68.75
Cell density (Cell/mL)	2.30×10^6
Response (PFU/mL)	4.7×10^7
Desirability	1.00

Abbreviations: DO, dissolved oxygen; PFU, plaque-forming unit.

Although BHK-21 culture in bioreactors and metabolism has been the subject of numerous publications (13, 14), integrated studies evaluating different bioreactors at different DO concentrations are rarely discussed. Perrin et al. have worked on the effect of culture media compositions on the vaccine but have not worked on the pH control mode (with or without base addition) and other unspecified modules. Using a central compound approach and a small number of experiments, the present work has shown that increasing cell density while decreasing pH, temperature, and DO during cell growth significantly increases virus yield (15).

The improvement of the nutrient media is the main focus of studies on the increase of virus yield in BHK-21 cell lines. Rarely are the effects of the physical environment and other important molecule concentrations, such as oxygen, pH, temperature, and cell density, investigated for this purpose. Therefore, to circumvent specific safety and production cost issues, the present study created an experimental rabies vaccine using BHK-21 grown in a serum-free medium (MDSS2). As a result, high upstream processes also necessitate a unique design for culture medium. Without affecting cell growth, the environmental factor should provide all the nutrients required (16). The high production of lactate and ammonium, metabolites responsible for pH decrease and growth inhibition, could be the cause of the earlier drop of initial pH (7.1) in Cruz et al.'s experiment with low values of maximum cell concentration (17).

To the best of our knowledge, this is the first study in which the optimization of veterinary rabies vaccine in BHK-21 cells is applied by a CCD. The typical result of a bioprocess screening experiment is that a subset of a few essential factors is identified. Process optimization based on a statistical method called response surface methodology (RSM) is a powerful experimental design tool to recognize the performance of composite systems (18). To find a theoretically ideal condition to maximize target production, the current study used a statistical analysis service (Design-Expert software from Stat-Ease Inc., USA). Typically, four variables can affect fermentation setup production (19).

The most popular optimization designs are Box-Behnken, central composite, and three-level complete factorial designs. A complete quadratic model can be fit by CCDs (17, 18). Because they can incorporate data from a properly planned factorial experiment, they are frequently used when the design plan calls for sequential experimentation (20). With a CCD, it is feasible to find a theoretically optimal state (combination of the factors) and identify the ignorance of specific aspects (from RSM) (21). In order to work with different regression models used in biological process studies, a center-rotation composite design was used as the experimental strategy (22). An analysis of variance (ANOVA) table was prepared to evaluate the importance of each factor and interaction. The variance of each parameter was calculated (23).

When pH and DO are kept constant at their midpoints, the answer falls with raising DO. The same is true for the influence of DO and cell density on virus yield. However, the response also increased as cell density did (24). In general, it can be determined from the contour and 3D plots that the following parameters have the greatest influence on the response:

Cell density > pH > temperature > DO

Due to the current study's limitations in checking the effective parameters in production, other modules, such as cell type and culture environment, can be used.

5.1. Conclusions

An appropriate cell substrate for producing robust rabies vaccines, which is the fundamental requirement for these vaccines' protective effect in humans, is the permanent BHK-21/C13 cell line used to manufacture the animal rabies vaccine. The technologies for BHK-21 cell culture and production are rather simple, and a concentration phase is not necessary for the manufacturing process. Therefore, the current study's data indicated that in order to maintain a high cell density of BHK-21 cells in the fermentor, the following parameters should be maintained:

pH = 7.21, temperature = 35.05°C, DO = 68.75%, and cell density = 2.30×10^6 cells/mL

Footnotes

Authors' Contribution: Study concept and design: Golshid Javdani and Nima Naseri; acquisition of the data: Rajab Mardani, Alireza Gholami; analysis and interpretation of the data: Golshid Javdani and Fatemeh Zali; drafting of the manuscript: Rajab Mardani; critical

References

1. Banyard AC, Tordo N. Rabies pathogenesis and immunology. *Rev Sci Tech*. 2018;**37**(2):323–30. [PubMed ID: 30747145]. https://doi.org/10.20506/rst.37.2.2805.

2. Liu C, Cahill JD. Epidemiology of rabies and current US vaccine guidelines. *R I Med J (2013)*. 2020;**103**(6):51–3. [PubMed ID: 32752569].

3. Rosatte RC, Donovan D, Davies JC, Brown L, Allan M, von Zuben V, et al. High-density baiting with ONRAB(R) rabies vaccine baits to control Arctic-variant rabies in striped skunks in Ontario, Canada. *J Wildl Dis*. 2011;**47**(2):459–65. [PubMed ID: 21441200]. https://doi.org/10.7589/0090-3558-47.2.459.

4. Shen CF, Lanthier S, Jacob D, Montes J, Beath A, Beresford A, et al. Process optimization and scale-up for production of rabies vaccine live adenovirus vector (AdRG1.3). *Vaccine*. 2012;**30**(2):300–6. [PubMed ID: 22079076]. https://doi.org/10.1016/j.vaccine.2011.10.095.

5. Simani S, Amirkhani A, Farahtaj F, Hooshmand B, Nadim A, Sharifian J, et al. Evaluation of the effectiveness of preexposure rabies vaccination in Iran. *Arch Iran Med*. 2004;**7**(4):251–5.

6. Cleaveland S, Barrat J, Barrat MJ, Selve M, Kaare M, Esterhuysen J. A rabies serosurvey of domestic dogs in rural Tanzania: results of a rapid fluorescent focus inhibition test (RFFIT) and a liquid-phase blocking ELISA used in parallel. *Epidemiol Infect*. 1999;**123**(1):157–64. [PubMed ID: 10487652]. [PubMed Central ID: PMC2810739]. https://doi.org/10.1017/s0950268899002563.

7. Johnston IC, ter Meulen V, Schneider-Schaulies J, Schneider-Schaulies S. A recombinant measles vaccine virus expressing wild-type glycoproteins: consequences for viral spread and cell tropism. *J Virol*. 1999;**73**(8):6903–15. [PubMed ID: 10400788]. [PubMed Central ID: PMC112775]. https://doi.org/10.1128/JVI.73.8.6903-6915.1999.

8. Momen SB, Siadat SD, Akbari N, Ranjbar B, Khajeh K. Applying central composite design and response surface methodology to optimize growth and biomass production of haemophilus influenzae type b. *Jundishapur J Microbiol*. 2016;**9**(6). e25246. [PubMed ID: 27630761]. [PubMed Central ID: PMC5011407]. https://doi.org/10.5812/jjm.25246.

9. Trabelsi K, Rourou S, Loukil H, Majoul S, Kallel H. Optimization of virus yield as a strategy to improve rabies vaccine production by Vero cells in a bioreactor. *J Biotechnol*. 2006;**121**(2):261–71. [PubMed ID: 16153733]. https://doi.org/10.1016/j.jbiotec.2005.07.018.

10. Jafari Harandi Z, Ghanavati Nasab S, Teimouri A. Synthesis and characterisation of magnetic activated carbon/diopside nanocomposite for removal of reactive dyes from aqueous solutions: experimental design and optimisation. *Int J Environ Anal Chem*. 2019;**99**(6):568–94. https://doi.org/10.1080/03067319.2019.1597867.

11. Goswami A, Plun-Favreau J, Nicoloyannis N, Sampath G, Siddiqui MN, Zinsou JA. The real cost of rabies post-exposure treatments. *Vaccine*. 2005;**23**(23):2970–6. [PubMed ID: 15811642]. https://doi.org/10.1016/j.vaccine.2004.12.008.

12. Souza RO, Henrique de Lima T, Orefice RL, de Freitas Araujo MG, de Lima Moura SA, Magalhaes JT, et al. Amphotericin B-loaded poly (lactic-co-glycolic acid) nanofibers: An alternative therapy scheme for local treatment of vulvovaginal candidiasis. *J Pharm Sci*. 2018;**107**(10):2674–85. [PubMed ID: 29940181]. https://doi.org/10.1016/j.xphs.2018.06.017.

13. Kallel H, Diouani MF, Loukil H, Trabelsi K, Snoussi MA, Majoul S, et al. Immunogenicity and efficacy of an in-house developed cell-culture derived veterinarian rabies vaccine. *Vaccine*. 2006;**24**(22):4856–62. [PubMed ID: 16600442]. https://doi.org/10.1016/j.vaccine.2006.03.012.

14. Lalosević D, Lalosević V, Lazarević-Ivanc L, Knezević I. BHK-21 cell culture rabies vaccine: immunogenicity of a candidate vaccine for humans. *Dev Biol (Basel)*. 2008;**131**:421–9. [PubMed ID: 18634504].

15. Perrin P, Madhusudana S, Gontier-Jallet C, Petres S, Tordo N, Merten OW. An experimental rabies vaccine produced with a new BHK-21 suspension cell culture process: use of serum-free medium and perfusion-reactor system. *Vaccine*. 1995;**13**(13):1244–50. [PubMed ID: 8578811]. https://doi.org/10.1016/0264-410x(94)00022-f.

16. Rafiee A, Ghanavati Nasab S, Teimouri A. Synthesis and characterization of pistachio shell/nanodiopside nanocomposite and its application for removal of Crystal Violet dye from aqueous solutions using central composite design. *Int J Environ Anal Chem*. 2019;**100**(14):1624–49. https://doi.org/10.1080/03067319.2019.1655556.

17. Cruz HJ, Freitas CM, Alves PM, Moreira JL, Carrondo MJ. Effects of ammonia and lactate on growth, metabolism, and productivity of BHK cells. *Enzyme Microb Technol*. 2000;**27**(1-2):43–52. [PubMed ID: 10862901]. https://doi.org/10.1016/s0141-0229(00)00151-4.

18. Ghanavati Nasab S, Semnani A, Karimi M, Javaheran Yazd M, Cheshmekhezr S. Synthesis of ion-imprinted polymer-decorated SBA-15 as a selective and efficient system for the removal and extraction of Cu(ii) with focus on optimization by response surface methodology. *Analyst*. 2019;**144**(15):4596–612. [PubMed ID: 31241069]. https://doi.org/10.1039/c9an00586b.

19. Ghanavati Nasab S, Semnani A, Teimouri A, Kahkesh H, Momeni Isfahani T, Habibollahi S. Removal of congo red from aqueous solution by hydroxyapatite nanoparticles loaded on zein as an efficient and green adsorbent: Response surface methodology and artificial neural network-genetic algorithm. *J Polym Environ*. 2018;**26**(9):3677–97. https://doi.org/10.1007/s10924-018-1246-z.

20. Fooladgar S, Teimouri A, Ghanavati Nasab S. Highly efficient removal of lead ions from aqueous solutions using chitosan/rice husk ash/nano alumina with a focus on optimization by response surface methodology: Isotherm, kinetic, and thermodynamic studies. *J Polym Environ*. 2019;**27**(5):1025–42. https://doi.org/10.1007/s10924-019-01385-3.

21. Nasab SG, Semnani A, Teimouri A, Yazd MJ, Isfahani TM, Habibollahi S. Decolorization of crystal violet from aqueous solutions by a novel adsorbent chitosan/nanodiopside using response surface methodology and artificial neural network-genetic algorithm. *Int J Biol Macromol*. 2019;**124**:429–43. [PubMed ID: 30452982]. https://doi.org/10.1016/j.ijbiomac.2018.11.148.

22. Ghanavati Nasab S, Teimouri A, Hemmasi M, Jafari Harandi Z, Javaheran Yazd M. Removal of Cd(II) ions from aqueous solutions by nanodiopside as a novel and green adsorbent: Optimisation by response surface methodology. *Int J Environ Anal Chem*. 2020;**101**(14):2128–49. https://doi.org/10.1080/03067319.2019.1699917.

23. Cruz HJ, Moreira JL, Carrondo MJ. Metabolically optimised BHK cell fed-batch cultures. *J Biotechnol*. 2000;**80**(2):109–18. [PubMed ID: 10908791]. https://doi.org/10.1016/s0168-1656(00)00254-6.

24. Visser JC, Dohmen WM, Hinrichs WL, Breitkreutz J, Frijlink HW, Woerdenbag HJ. Quality by design approach for optimizing the formulation and physical properties of extemporaneously prepared orodispersible films. *Int J Pharm*. 2015;**485**(1-2):70–6. [PubMed ID: 25746737]. https://doi.org/10.1016/j.ijpharm.2015.03.005.